Received: 6 June 2017 | Revised: 5 October 2017 | Accepted: 15 November 2017 | Published on: 10 January 2018

DOI: 10.1002/asl.798

Atmospheric Science Letters RMetS

RESEARCH ARTICLE

# Evidence of convective transport in tropical West Pacific region during SHIVA experiment

Gisèle Krysztofiak[1] | Valéry Catoire[1] | Paul D. Hamer[2*] | Virginie Marécal[2] | Claude Robert[1] | Andreas Engel[3] | Harald Bönisch[3†] | Katja Grossmann[4‡] | Birgit Quack[5] | Elliot Atlas[6] | Klaus Pfeilsticker[4]

[1]LPC2E, Université Orléans – CNRS (UMR 7328), Orléans Cedex 2, France

[2]CNRM, Météo-France – CNRS (UMR 3589), Toulouse Cedex, France

[3]Department of Experimental Atmospheric Research, Institute of Atmospheric and Environmental Science, J. W. Goethe-University Frankfurt am Main, Frankfurt am Main, Germany

[4]Chemical Oceanography Department, Institute of Environmental Physics, Ruprecht-Karls-Universität Heidelberg, Germany

[5]GEOMAR Helmholtz Centre for Ocean Research Kiel, Germany

[6]Department of Atmospheric Sciences, Rosenstiel School for Marine and Atmospheric Sciences, Miami, Florida

**Correspondence**
G. Krysztofiak, Laboratoire de Physique et Chimie de l'Environnement et de l'Espace, Université d' Orléans CNRS (UMR 7328), 3A Avenue de la Recherche Scientifique, 45071 Orléans Cedex 2, France.
Email: gisele.krysztofiak@cnrs-orleans.fr

Air masses in the convective outflows of four large convective systems near Borneo Island in Malaysia were sampled in the height range 11–13 km within the frame of the SHIVA (Stratospheric Ozone: Halogen Impacts in a Varying Atmosphere) FP7 European project in November and December 2011. Correlated enhancements of CO, $CH_4$ and the short-lived halogen species ($CH_3I$ and $CHBr_3$) were detected when the aircraft crossed the anvils of the four systems. These enhancements were interpreted as the fingerprint of vertical transport from the boundary layer by the convective updraft and then horizontal advection in the outflow. For the four observations, the fraction $f$ of air from the boundary layer ranged between 15 and 67%, showing the variability in transport efficiency depending on the dynamics of the convective system.

KEYWORDS

aircraft, convective transport, *in situ* measurements, VSLS transport

## 1 | INTRODUCTION

The composition of the tropical upper troposphere (UT) is affected by the efficiency of the convective transport of chemical species (Fueglistaler et al., 2009). Tropical deep convection can efficiently transport surface emitted compounds from the lower troposphere into the tropical tropopause layer (TTL) altitude range (Marécal, Rivière, Held, Cautenet, & Freitas, 2006). Since in tropical regions large emissions of halogenated very short-lived species (VSLS) coincide with deep convection, one may expect rapid transport of VSLS into the TTL. Indeed, an efficient transport of chemical tracers from polluted air masses (Bechara, Borbon, Jambert, Colomb, & Perros, 2010) or biogenic sources from the oceans such as halogenated VSLS ($CHBr_3$, $CH_2Br_2$, $CH_3I$, etc.: Sala et al., 2014; Tegtmeier et al., 2013) was observed and modelled (Navarro et al., 2015; Werner et al., 2017).

In the last decades, several field campaigns (such as SHIVA—Stratospheric Ozone: Halogen Impacts in a Varying Atmosphere, Sala et al., 2014; Fuhlbrügge et al., 2016;

---

[*] Current address: NILU, PO Box 100, NO-2027 Kjeller, Norway.

[†] Current address: Institute for Meteorology and Climate Research, Karlsruhe Institute of Technology, Karlsruhe, Germany.

[‡] Current address: Joint Institute for Regional Earth System Science and Engineering (JIFRESSE), University of California Los Angeles, Los Angeles, CA 90095.

TC4 [www.nasa.gov/mission_pages/TC4]; ATTREX, Jensen et al., 2015) and modelling studies (Hossaini et al., 2012) focused on determining the contribution of the VSLS to the bromine burden in the upper troposphere and lower stratosphere (UTLS). Observational campaigns can only address the transport into the UT on an event-like basis but they are of high interest because the convection parameterisation is a major source of uncertainty in chemistry transport models (Arteta, Marécal, & Rivière, 2009; Hoyle et al., 2011). Previous observational studies of convective outflows at mid-latitudes (Bertram et al., 2007) and in the tropics (Ray et al., 2004) reported an effective transport of short-lived trace gases (Bechara et al., 2010; Cohan, Schultz, Jacob, Heikes, & Blake, 1999) by convection from the boundary layer (BL) into the UT. These studies showed that a fraction of 20–40% of BL air was present in individual convective plumes transported rapidly to the UT.

One of the objectives of the SHIVA FP7 European project was the investigation of the atmospheric transport of VSLS from the BL into the UTLS. The campaign took place in the tropical West Pacific during the boreal winter monsoon in November and December 2011 when strong convective transport is expected to occur (e.g., Aschmann, Sinnhuber, Atlas, & Schauffler, 2009; Levine, Braesicke, Harris, Savage, & Pyle, 2007; Liang et al., 2014). Here, we present airborne measurements for four mesoscale convective events indicating enhanced UT CO and $CH_4$ volume mixing ratios (vmr) that directly correlate with $CHBr_3$ and $CH_3I$ enhancements when the aircraft passed the anvil of convective cumulus clouds. The fraction of air originating from the BL is calculated by analysis of the CO enhancements.

The SHIVA campaign and instruments are presented in Section 2. In Section 3, we discuss the meteorological conditions of the flights and the detection of convective transport and its influence on CO and $CH_4$ concentrations. Implications for the vertical transport for VSLS are also addressed. Section 4 concludes the study.

## 2 | SHIVA FIELD CAMPAIGN AND MEASUREMENTS

### 2.1 | Measurement campaign

The SHIVA aircraft campaign took place in Malaysia between November 16 and December 11, 2011. Using the German Aerospace agency (DLR) Falcon-20 aircraft, 16 research flights were conducted from Miri (Malaysia) airport in northwestern Borneo. In the present study, the results of four flights performed on November 19 (F19NOV), December 9, 2011 (F09DEC) and two on December 11 (F11DECa and F11DECb) are described in Appendix S1 (Supporting Information). The RV *Sonne* cruise started on November 15 in Singapore, passed near the northern coast of Borneo and ended in Manila, Philippines on November 29. Measurements on *Sonne* are used to estimate the variability of halocarbons concentration in the BL.

### 2.2 | Experimental method

The airborne CO and $CH_4$ measurements were performed with the SPIRIT instrument (Catoire et al., 2017), and $CHBr_3$ and $CH_3I$ with the GHOST instrument (Sala et al., 2014). Additionally, whole air samples taken in the RV Sonne were analysed for halocarbons, CO and $CH_4$. More detail about instrumentation is provided in Appendix S1. Relative humidity from the Falcon-20 instrument and webcam imagery from mini-DOAS instrument (Großmann, 2014) are used to study the convective condition.

## 3 | RESULTS AND DISCUSSION

### 3.1 | Meteorological situation of the flights

Figure 1 depicts the flight tracks together with the brightness temperatures measured by the 11-μm channel IR108 from on board the Japanese geostationary satellite MTSAT-2. Additionally, cloud height is determined based on Hamada and Nishi (2010) and Iwasaki et al. (2010) (not shown).

Figure 1(a) indicates the presence of a well-developed convective system around 6°N and 115.5°E during research flight F19NOV that reached a maximum height of ~16 ± 0.5 km in altitude with an extended anvil on its west side reaching 14.5 ± 0.5 km. For F09DEC, a convective system with a smaller horizontal extent was detected at around 5.5°N and 118.5°E (Figure 1(b)). The convective part of the system reached ~15.5 ± 1 km altitude and was embedded in stratiform clouds with maximum height ~13.5 ± 1.5 km. In F11DECa (Figure 1(c)), a well-developed convective system was probed between 1°–2°N and 106°–107°E. The cloud top altitude for this system reached a maximum of ~17 ± 0.5 km. The convection cell lasted throughout the day and was again probed during the back flight from Singapore to Miri in the afternoon for F11DECb (Figure 1(d)), though with a weakened strength.

### 3.2 | Impact of deep convection on trace gases

#### 3.2.1 | CO and $CH_4$

Figures 2–4 show CO and $CH_4$ measured by the SPIRIT instrument. In all cases when the aircraft crossed convective outflows (period determined by webcam data, relative humidity and brightness temperature, see Figure 2), the mixing ratios of the measured tracers are increased. In the next section, such measurements are defined as $[X]_{\mathrm{UTconv}}$, and the lower tracer mixing ratios observed outside of the convective system are defined as $[X]_{\mathrm{UT}}$. CO and $CH_4$ are mainly emitted from anthropogenic sources in the BL. The sudden increases of $[X]_{\mathrm{UTconv}}$, larger than the UT mixing ratios ($[X]_{\mathrm{UT}}$), i.e., between 15 and 60 pbbv for CO and

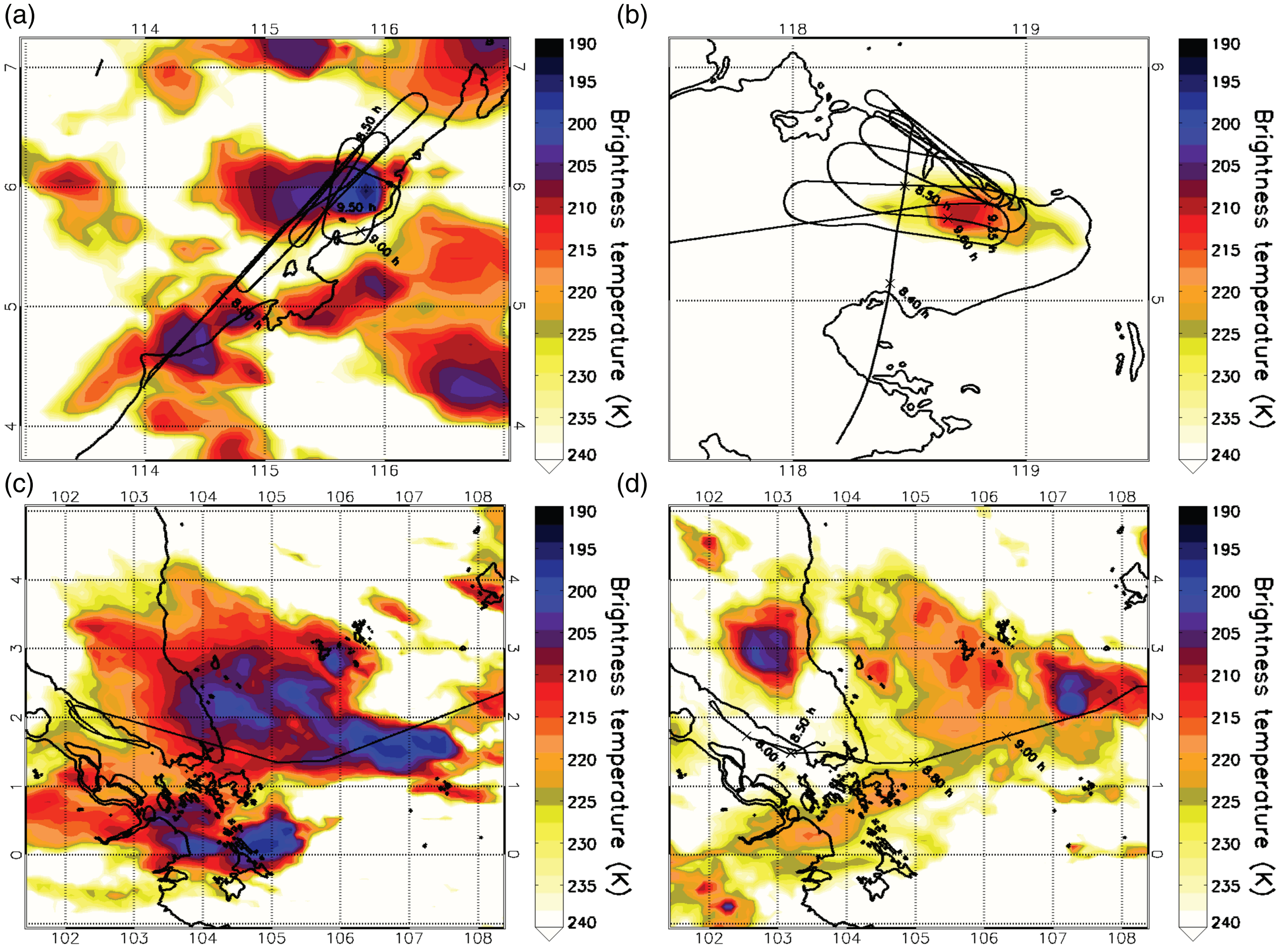

**FIGURE 1** IR brightness temperature from MTSAT-2 channel IR108 (10.3–11.3 μm) for 0900 UTC on November 19, 2011 (a), 0900 UTC 9 December 2011 (b), 0400 UTC December 11, 2011 (c) and 0900 UTC on 11 December 2011 (d). The flight tracks are displayed as black lines

between 20 and 50 ppbv for $CH_4$, are thus indicative of transport of polluted air from the BL into the UT. Such enhancements of BL tracers due to convection and affecting the UT composition have also been previously reported by Bechara et al. (2010) and Borbon et al. (2012).

### 3.2.2 | Fraction of BL air detected in the UT

CO has proven to be a particularly good tracer to study convection due to its source at the surface and tropospheric lifetime of 1–3 months (Dessler, 2002). Following Bertram et al. (2007), the measured tracer's mixing ratio $[X]$ is used to quantify the air fraction $f$ originating from the BL and transported by convection, using the following equation:

$$[X]_{\mathrm{UTconv}} = f.[X]_{\mathrm{BL}} + (1-f).[X]_{\mathrm{UT}} \qquad (1)$$

where $[X]_{BL}$ represents the vmr of the tracer in the BL. For the air masses affected by convection, $[X]_{\mathrm{UTconv}}$ is determined from the calculated means for $CH_4$ and CO. For F19NOV, $[X]_{\mathrm{BL}}$ is determined from the air directly probed below the convective system during the take-off and landing since the convective system was located near Miri. For F09DEC, the surface air was directly sampled during a dive under the convective system down to 1 km altitude and for F11DECa and F11DECb, the BL measurements from RV *Sonne* are used. All relevant parameters are summarised in Table 1. In all, 18–50% of air present in the outflow of convective systems was recently transported from the BL, based on measured CO and $CH_4$.

### 3.2.3 | Impact of deep convection on upper tropospheric $CH_3I$ and $CHBr_3$

For the four studied flights, Figures 2–4 (upper panel) show GHOST-MS measurements of $CHBr_3$ and $CH_3I$ for air affected by deep convection. As for $CH_4$ and CO, flight-dependent enhancements ranging from 0.3 to 0.5 pptv for $CH_3I$ and 0.6–1.0 pptv for $CHBr_3$ are observed in the air of convective outflow.

Three areas are defined in order to calculate the BL mean concentration depending on the location of the flight by using a combination of GHOST and RV *Sonne* measurements. For F19NOV, $[X]_{\mathrm{BL}}$ only takes into account measurements in the region northeast of Miri, for F09DEC the region on the eastern side of Borneo and for F11DEC the region east of Singapore. Averaging over the designated areas separately removes the

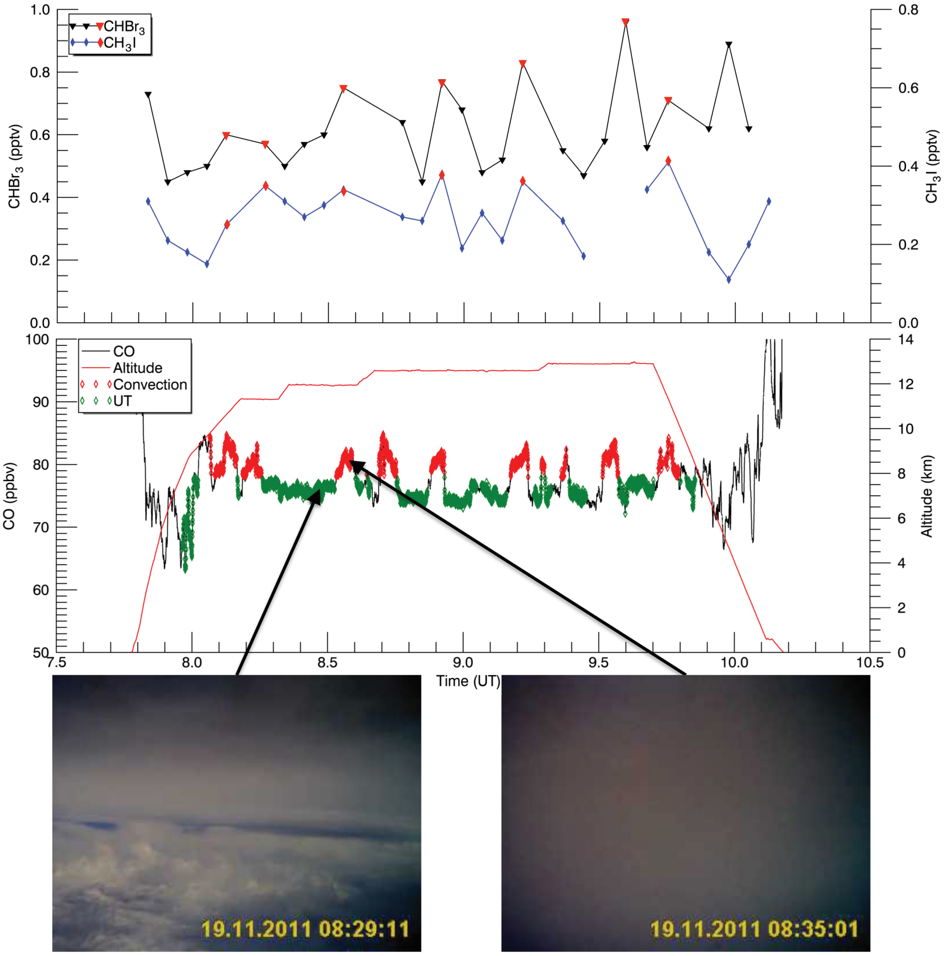

**FIGURE 2** Measurements from aboard the Falcon-20 during SHIVA campaign during the afternoon flight on November 19, 2011. From bottom to top: mini-DOAS webcam picture, CO (in black) and altitude (in red) from SPIRIT instrument and CHBr3 (in black triangles) and CH3I (in blue lozenge) from GHOST-MS instrument. The times when the aircraft crossed the anvil cloud were determined according to the mini-DOAS webcam, the humidity data from the Falcon aircraft (showing that when the Falcon penetrating the clouds the relative humidity exceeded 100% that is indicative of supersaturated air), and the brightness temperature of the cloud area inferred from the MTSAT (for data lower than 225 K, equivalent to 13 km). In panels, these data are labelled in red. Measurements taken into account to calculate $[X]_{\mathrm{CONV}}$ are labelled in red and for $[X]_{\mathrm{UT}}$ in green

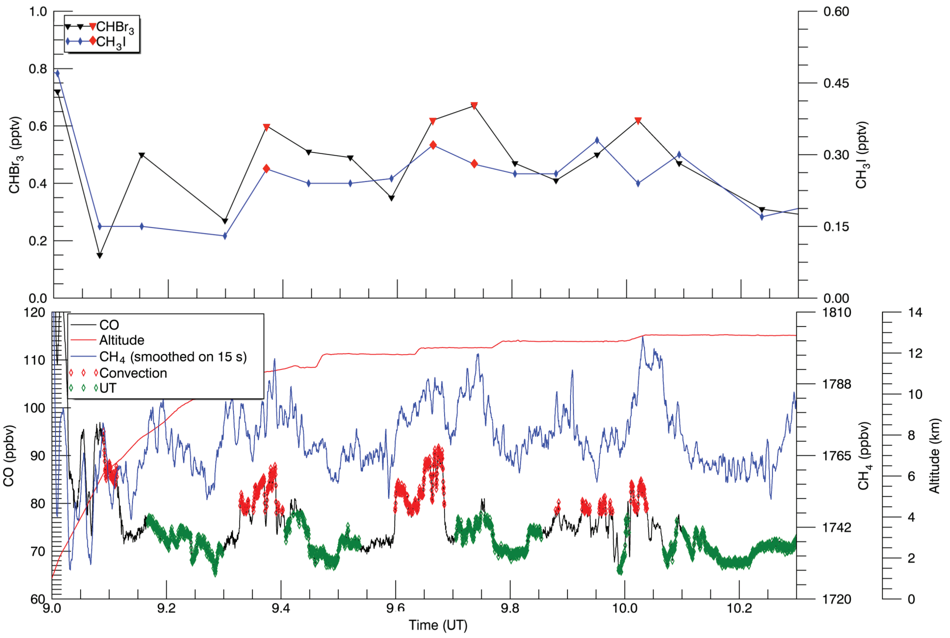

**FIGURE 3** Same as Figure 2 but for the flight on the afternoon flight on December 9, 2011. In the bottom panel, the blue line shows the CH4 measurements of SPIRIT

variability in oceanic emission sources between each region. For $CHBr_3$, it results in averaged concentrations in the range 1.8–2.7 pptv and for $CH_3I$ in the range 0.3–0.5. The UT concentrations are calculated individually for each flight and give concentrations in the range 0.39–0.52 pptv for $CHBr_3$ and 0.21–0.25 pptv for $CH_3I$. According to Sala et al. (2014), the mean concentration of $CHBr_3$ in the UT is 0.61 ± 0.2 pptv and the mean concentration in the BL is 1.43 ± 0.53 pptv, considering data from all SHIVA flights in the tropics. However, the reported mean concentration for UT also contains the measurements affected by convection. For F19NOV, F09DEC and F11DEC, the resulting fractions *f* using $CHBr_3$ and $CH_3I$

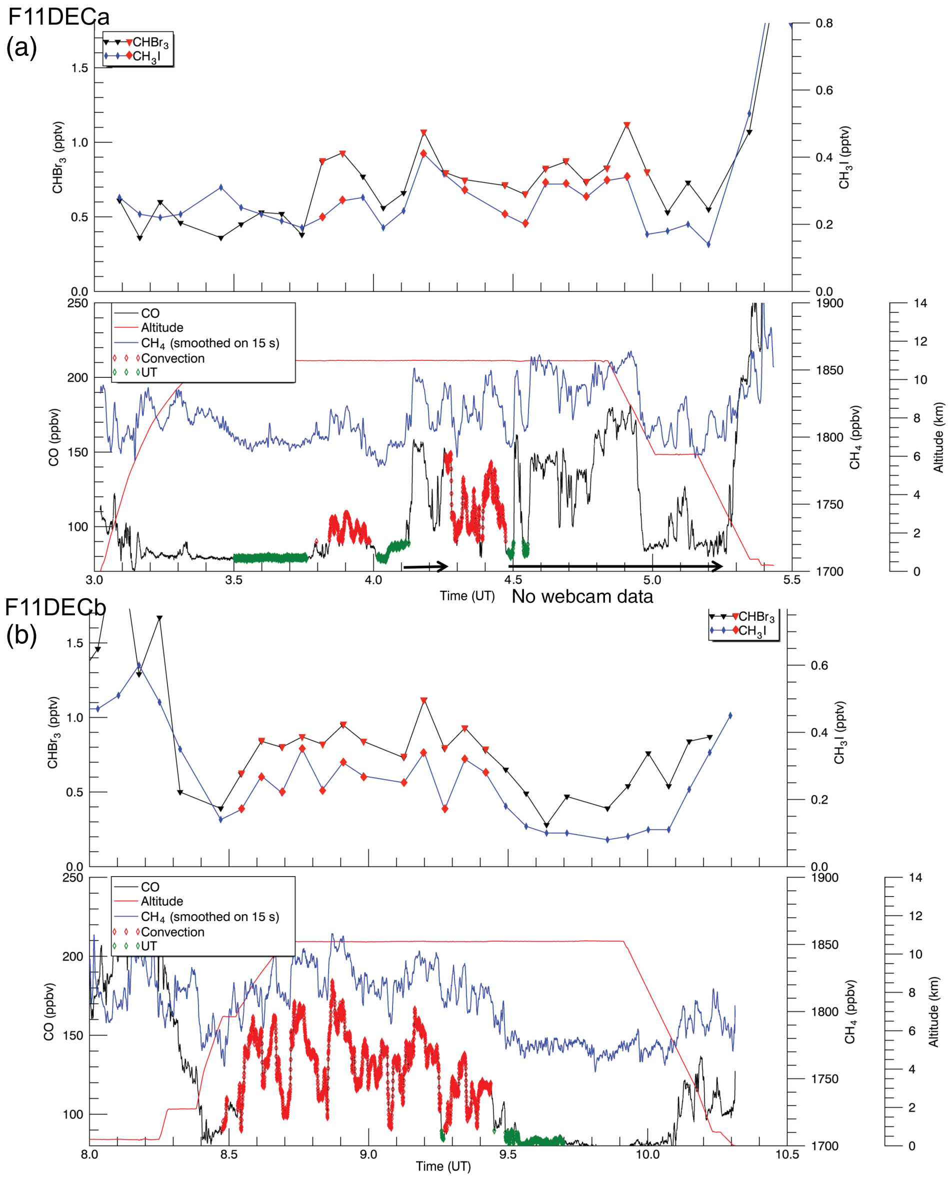

**FIGURE 4** Same as Figures 2 and 3 but for the morning and afternoon flights on December 11, 2011

are in the range between 15 and 67%. Table 1 summarises measured and averaged mixing ratios of all gases and fractions *f* for $CHBr_3$ and $CH_3I$. Note, the calculated fractions *f* depend on the actual source strength at the marine boundary surface, which for $CHBr_3$ are known to strongly vary in space and time. Furthermore, since the time resolution of the $CHBr_3$ and $CH_3I$ measurements is longer than for CO and $CH_4$ measurements, the different averaging time may also affect the inferred fractions *f* by probably biasing them low relative to *f* calculated from other trace gases.

### 3.2.4 | Comparison with previous studies

Considering all species from all flights, a mean fraction of 29 ± 25% is obtained (mean of the fractions *f* with standard deviations $\sigma < 0.4$). Table 1 compares our inferred fractions *f* with those found in the literature. The inferred mean fraction *f* derived from CO and $CH_4$ (18–50%) is in reasonable agreement with the fraction *f* inferred by Bertram et al. (2007), Ray et al. (2004), Lopez et al. (2006) and Bechara et al. (2010) given the range uncertainties. Like in our study, these authors used CO and $CH_4$ measurements among other tracers to calculate the fractions *f*. The fractions of Cohan et al. (1999) and Barth et al. (2016) using VSLS $CH_3I$, $CH_3O_2H$, $CHBr_3$ and VOCs are in agreement with our results (15–67%) derived from $CHBr_3$ and $CH_3I$.

Also, from the previous studies related to SHIVA project, Großmann (2014) inferred a fraction of 19% for the short-lived species HCHO measured during F19NOV using a mini-DOAS instrument (Stutz et al., 2017) and Fuhlbrügge et al. (2016) calculated similar contributions of marine BL air to the free troposphere (30–50%) up to 13 km height for the whole SHIVA-campaign with a trajectory model, again in agreement with the results of the present study.

## 4 | CONCLUSIONS

Within the frame of the SHIVA project, air of the anvil from mesoscale large convective systems was sampled at altitudes

**TABLE 1** SPIRIT measured mean mixing ratios of CO, $CH_4$, $CHBr_3$ and $CH_3I$ for the boundary layer ($[X]_{BL}$), upper troposphere ($[X]_{UT}$) and convective air masses ($[X]_{UTconv}$) during the flights on November 19, 2011, December 9, 2011 and December 11, 2011

| | | | $[X]_{BL}$[a] | $[X]_{UT}$[a] | $[X]_{UTconv}$[a] | fraction $f$[b] | Comment |
|---|---|---|---|---|---|---|---|
| This study | F19NOVb | CO[c] | 95 ± 12 | 76 ± 2 | 81 ± 1 | 0.26 ± 0.21 | Borneo region (6°N–117°E) |
| | | $CHBr_3$[d] | 1.82 ± 0.86 | 0.51 ± 0.04 | 0.73 ± 0.12 | 0.17 ± 0.15 | |
| | | $CH_3I$[d] | 0.43 ± 0.17 | 0.24 ± 0.06 | 0.35 ± 0.05 | 0.59 ± 0.70 | |
| | F09DECb | CO[c] | 129 ± 9 | 73 ± 3 | 83 ± 3 | 0.18 ± 0.08 | |
| | | $CH_4$[c] | 1801 ± 25 | 1771 ± 11 | 1782 ± 10 | 0.37 ± 0.60 | |
| | | $CHBr_3$[d] | 2.32 ± 1.66 | 0.39 ± 0.12 | 0.69 ± 0.03 | 0.16 ± 0.15 | |
| | | $CH_3I$[d] | 0.52 ± 0.54 | 0.22 ± 0.06 | 0.28 ± 0.03 | 0.20 ± 0.43 | |
| | F11DECa | CO[c] | 179 | 81 ± 3 | 109 ± 15 | 0.29 ± 0.16 | |
| | | $CH_4$[c] | 1868 | 1794 ± 6 | 1817 ± 13 | 0.31 ± 0.20 | |
| | | $CHBr_3$[d] | 2.71 ± 0.89 | 0.50 ± 0.1 | 0.84 ± 0.13 | 0.15 ± 0.10 | |
| | | $CH_3I$[d] | 0.32 ± 0.02 | 0.23 ± 0.04 | 0.29 ± 0.07 | 0.67 ± 0.96 | |
| | F11DECb | CO[c] | 179 | 83 ± 2 | 131 ± 20 | 0.50 ± 0.21 | |
| | | $CH_4$[c] | 1868 | 1776 ± 8 | 1822 ± 16 | 0.50 ± 0.20 | |
| | | $CHBr_3$[d] | 2.71 ± 0.89 | 0.51 ± 0.16 | 0.84 ± 0.12 | 0.15 ± 0.11 | |
| | | $CH_3I$[d] | 0.32 ± 0.02 | 0.21 ± 0.03 | 0.27 ± 0.06 | 0.55 ± 0.35 | |
| | Mean | | | | | 0.29 ± 0.25[e] | |
| Cohan et al. (1999) | | | | | | 0.36–0.68 | South Pacific (60°S–10°N) |
| Ray et al. (2004) | | | | | | 0.20–0.45 | Mexican Gulf (20°N) |
| Lopez et al. (2006) | | | | | | 0.2–0.4 | Subtropical, Florida |
| Bertram et al. (2007) | | | | | | 0.17 ± 0.08 | Eastern United States and Canada |
| Bechara et al. (2010) | | | | | | 0.40 ± 0.15 | West Africa |
| Großmann (2014) | | | | | | 0.19 | Borneo region |
| Derived from Barth et al. (2016) | | | | | | 0.27–0.58 | Oklahoma and northeast Colorado |

These inferred vmr are used in the calculation of the fraction $f$ of air coming from the boundary layer detected in the convective air mass. The mean fraction $f$ found is compared with other studies.

[a] Uncertainties are $1\sigma$ on the mean.

[b] Uncertainties include propagation error of the standard deviation of individual values.

[c] Volume mixing ratio in ppbv.

[d] Volume mixing ratio in pptv.

[e] Mean of the fraction $f$ with standard deviations $\sigma < 0.4$.

around 11–13 km near Borneo (6.0°N–115.5°E and 5.5°N–118.5°E) and Singapore (1°N–106°E) on November 19, December 9 and 11, 2011, respectively. Correlated measurements of CO, $CH_4$, $CHBr_3$ and $CH_3I$ were interpreted with respect to the strength of air mass transported from the BL to the UT by convective systems. The fraction $f$ of BL air contained in the fresh convective outflow was calculated to range between 18 and 50% based on measured CO and $CH_4$. Correlative measurements of $CHBr_3$ and $CH_3I$ indicated a fraction between 15 and 67%. The inferred range of $f$ indicates the variability in mixing due to air mass entrainment into the convective system, but also points to limitations in the method due to its dependence on the variability of the tracer's source strength and lifetime of the species.

To go a step further, modelling or measurements from higher flying platforms, such as recently performed from the Global Hawk in the NASA ATTREX project over the Pacific, may provide estimates of the transport of halogenated VSLS due to deep convection reaching the TTL (e.g., Werner et al., 2017).

## ACKNOWLEDGEMENTS

The contributions of S. Chevrier, L. Pomathiod, G. Chalumeau and K. Le Letty for engineering and construction of the SPIRIT instrument and for operations during the campaign are gratefully acknowledged. For GhOST-MS, the contributions of T. Keber and S. Sala to the successful measurements are gratefully acknowledged. This study has been possible thanks to funding provided by the EU project SHIVA (FP7-ENV-2007-1-226224), from the Deutsche Forschungsgemeinschaft (DFG) through grants PF384/9-1, 9-2, EN367/5-1 and EN367/5-2, the Federal Ministry of Education and Research (BMBF) grants 03G0218A and 03F0611A, the NASA grant NNX12AH02G and the Labex Voltaire program (ANR-10-LABX-100-01). The CTOP data were collected and distributed by Research Institute for Sustainable Humanosphere, Kyoto University, Japan.

## REFERENCES

Arteta, J., Marécal, V., & Rivière, E. D. (2009). Regional modelling of tracer transport by tropical convection. Part 1: Sensitivity to convection parameterization. *Atmospheric Chemistry and Physics*, *9*, 7081–7100.

Aschmann, J., Sinnhuber, B.-M., Atlas, E. L., & Schauffler, S. M. (2009). Modeling the transport of very short-lived substances into the tropical upper troposphere and lower stratosphere. *Atmospheric Chemistry and Physics*, *9*, 9237–9247. https://doi.org/10.5194/acp-9-9237-2009

Barth, M. C., Bela, M. M., Fried, A., Wennberg, P. O., Crounse, J. D., St. Clair, J. M., … Cantrell, C. A. (2016). Convective transport of peroxides by thunderstorms observed over the Central U.S. during DC3. *Journal of Geophysical Research – Atmospheres*, *121*, 4272–4295. https://doi.org/10.1002/2015JD024570

Bechara, J., Borbon, A., Jambert, C., Colomb, A., & Perros, P. E. (2010). Evidence of the impact of deep convection on reactive volatile organic compounds in the upper tropical troposphere during the AMMA experiment in West Africa. *Atmospheric Chemistry and Physics*, *10*, 10321–10334. https://doi.org/10.5194/acp-10-10321-2010

Bertram, T. H., Perring, A. E., Wooldridge, P. J., Crounse, J. D., Kwan, A. J., Wennberg, P. O., … Cohen, R. C. (2007). Direct measurements of the convective recycling of the upper troposphere. *Science*, *315*, 816–820.

Borbon, A., Ruiz, M., Bechara, J., Aumont, B., Chong, M., Huntrieser, H., … Perros, P. E. (2012). Transport and chemistry of formaldehyde by mesoscale convective systems in West Africa during AMMA 2006. *Journal of Geophysical Research*, *117*, D12301. https://doi.org/10.1029/2011JD017121

Catoire, V., Robert, C., Chartier, M., Jacquet, P., Guimbaud, C., & Krysztofiak, G. (2017). The SPIRIT airborne instrument: A three-channel infrared absorption spectrometer with quantum cascade lasers for in-situ atmospheric trace-gas measurements. *Applied Physics B*, *123*, 244. https://doi.org/10.1007/s00340-017-6820-x

Cohan, D. S., Schultz, M. G., Jacob, D. J., Heikes, B. G., & Blake, D. R. (1999). Convective injection and photochemical decay of peroxides in the tropical upper troposphere: Methyl iodide as a tracer of marine convection. *Journal of Geophysical Research*, *104*, 5717–5724.

Dessler, A. E. (2002). The effect of deep, tropical convection on the tropical tropopause layer. *Journal of Geophysical Research*, *107*, 2156–2202. https://doi.org/10.1029/2001JD000511

Fueglistaler, S., Dessler, A. E., Dunkerton, T. J., Folkins, I., Fu, Q., & Mote, P. W. (2009). Tropical tropopause layer. *Reviews of Geophysics*, *47*, RG1004. https://doi.org/10.1029/2008RG000267

Fuhlbrügge, S., Quack, B., Tegtmeier, S., Atlas, E., Hepach, H., Shi, Q., … Krüger, K. (2016). The contribution of oceanic halocarbons to marine and free tropospheric air over the tropical West Pacific. *Atmospheric Chemistry and Physics*, *16*, 7569–7585. https://doi.org/10.5194/acp-16-7569-2016

Großmann, K. (2014). *Aircraft-borne DOAS limb observations of UV/visible absorbing trace gas species over Borneo: Implications for the photochemistry of iodine, volatile organic oxide degradation, and lightning-produced radicals*. Heidelberg: University of Heidelberg.

Hamada, A., & Nishi, N. (2010). Development of a cloud-top height estimation method by geostationary satellite split-window measurements trained with CloudSat data. *Journal of Applied Meteorology and Climatology*, *49*, 2035–2049.

Hossaini, R., Chipperfield, M. P., Feng, W., Breider, T. J., Atlas, E., Montzka, S. A., … Elkins, J. (2012). The contribution of natural and anthropogenic very short-lived species to stratospheric bromine. *Atmospheric Chemistry and Physics*, *12*, 371–380. https://doi.org/10.5194/acp-12-371-2012

Hoyle, C. R., Marécal, V., Russo, M. R., Allen, G., Arteta, J., Chemel, C., … Zeng, G. (2011). Representation of tropical deep convection in atmospheric models. Part 2: Tracer transport. *Atmospheric Chemistry and Physics*, *11*, 8103–8131.

Iwasaki, S., Shibata, T., Nakamoto, J., Okamoto, H., Ishimoto, H., & Kubota, H. (2010). Characteristics of deep convection measured by using the A-train constellation. *Journal of Geophysical Research*, *115*, D06207. https://doi.org/10.1029/2009JD013000

Jensen, E. J., Pfister, L., Jordan, D. E., Bui, T. V., Ueyama, R., Singh, H. B., … Pfeilsticker, K. (2015). The NASA Airborne Tropical TRopopause EXperiment (ATTREX): High-altitude aircraft measurements in the tropical Western Pacific. *Bulletin of the American Meteorological Society*, *12/2015*: 129–144. https://doi.org/10.1175/BAMS-D-14-00263.1

Levine, J. G., Braesicke, P., Harris, N. R. P., Savage, N. H., & Pyle, J. A. (2007). Pathways and timescales for troposphere-to-stratosphere transport via the tropical tropopause layer and their relevance for very short lived substances. *Journal of Geophysical Research*, *112*, D04308. https://doi.org/10.1029/2005JD006940

Liang, Q., Atlas, E., Blake, D., Dorf, M., Pfeilsticker, K., & Schauffler, S. (2014). Convective transport of very short lived bromo-carbons to the stratosphere. *Atmospheric Chemistry and Physics*, *14*, 5781–5792. https://doi.org/10.5194/acp-14-5781-2014

Lopez, J. P., Fridlind, A. M., Jost, H.-J., Loewenstein, M., Ackerman, A. S., Campos, T. L., … Herman, R. L. (2006). CO signatures in subtropical convective clouds and anvils during CRYSTAL-FACE: An analysis of convective transport and entrainment using observations and a cloud-resolving model. *Journal of Geophysical Research*, *111*, D09305. https://doi.org/10.1029/2005JD006104

Marécal, V., Rivière, E. D., Held, G., Cautenet, S., & Freitas, S. (2006). Modelling study of the impact of deep convection on the UTLS air composition. Part I: Analysis of ozone precursors. *Atmospheric Chemistry and Physics*, *6*, 1567–1584.

Navarro, M. A., Atlas, E. L., Saiz-Lopez, A., Rodriguez-Lloveras, X., Kinnison, D. E., Lamarque, J.-F., … Donets, V. (2015). Airborne measurements of organic bromine compounds in the Pacific tropical tropopause layer. *Proceedings of the National Academy of Sciences of the United States of America*, *112*, 13789–13793. https://doi.org/10.1073/pnas.1511463112

Ray, E. A., Rosenlof, K. H., Richard, E. C., Hudson, P. K., Cziczo, D. J., Loewenstein, M., …. Herman R. L. (2004). Evidence of the effect of summertime midlatitude convection on the subtropical lower stratosphere from CRYSTAL-FACE tracer measurements. *Journal of Geophysical Research*, *109*, D18304. https://doi.org/10.1029/2004JD004655

Sala, S., Bönisch, H., Keber, T., Oram, D. E., Mills, G., & Engel, A. (2014). Deriving an atmospheric budget of total organic bromine using airborne in situ measurements from the western Pacific area during SHIVA. *Atmospheric Chemistry and Physics*, *14*, 6903–6923. https://doi.org/10.5194/acp-14-6903-2014

Stutz, J., Werner, B., Spolaor, M., Scalone, L., Festa, J., Tsai, C., … Pfeilsticker, K. (2017). A new differential optical absorption spectroscopy instrument to study atmospheric chemistry from a high-altitude unmanned aircraft. *Atmospheric Measurement Techniques*, *10*, 1017–1042. https://doi.org/10.5194/amt-10-1017-2017

Tegtmeier, S., Krüger, K., Quack, B., Atlas, E., Blake, D. R., Boenisch, H., … Ziska, F. (2013). The contribution of oceanic methyl iodide to stratospheric iodine. *Atmospheric Chemistry and Physics*, *13*, 11869–11886. https://doi.org/10.5194/acp-13-11869-2013

Werner, B., Stutz, J., Spolaor, M., Scalone, L., Raecke, R., Festa, J., … Pfeilsticker, K. (2017). Probing the subtropical lowermost stratosphere and the tropical upper troposphere and tropopause layer for inorganic bromine. *Atmospheric Chemistry and Physics*, *17*, 1161–1186. https://doi.org/10.5194/acp-17-1161-2017

## SUPPORTING INFORMATION

Additional Supporting Information may be found online in the supporting information tab for this article.

**How to cite this article:** Krysztofiak G, Catoire V, Hamer PD, et al. Evidence of convective transport in tropical West Pacific region during SHIVA experiment. *Atmos. Sci. Lett.* 2018;19:e798. https://doi.org/10.1002/asl.798